



# A hybrid legged-wheeled obstacle avoidance strategy for service operations

Ernesto Christian Orozco-Magdaleno<sup>1</sup> · Daniele Cafolla<sup>2</sup> · Eduardo Castillo-Castañeda<sup>1</sup> · Giuseppe Carbone<sup>3</sup>

Received: 20 November 2019 / Accepted: 30 January 2020 / Published online: 3 February 2020  
© Springer Nature Switzerland AG 2020

## Abstract

Hybrid legged-wheeled robots are gaining interest in various service applications, like surveillance or inspection in hospitals. The autonomy of these robots is not only related to their power consumption, it mostly refers to their capability to safely move in complex partially structured environments. This paper proposes to investigate the combination of different moving strategies and sensors to enhance the adaptability and autonomy of a hybrid hexapod robot in specific environments shared with humans. Namely, this paper proposes a locomotion strategy that combines leg motions and Mecanum omniwheels with multiple sensory feedbacks to achieve safe obstacle avoidance during a service operation. Several experimental tests are carried out by using Cassino Hexapod III in combination with sonar, IMU and Lidar sensors at IRCCS Neuromed site in Pozzilli. Experimental results show the effectiveness of the proposed operation strategy with Cassino Hexapod III to avoid multiple obstacles.

**Keywords** Obstacle avoidance · Mobile robot · Experimental robotics · Service robotics

## 1 Introduction

In the last years many service operations are requiring a higher degree of autonomy of the service robots to have a better performance and autonomy. These service operations are tasks where the robot needs to interact with the environment, facing obstacles, people or the rough terrains [1]. Thus, the autonomy is becoming one of the main features for service robots to carry out surveillance tasks in a hospital, inspection/maintenance operations in cultural heritage buildings or extraterrestrial service tasks in Mars [2]. Nowadays, the autonomy of a service robot does not only mean its operation time, it also means that the robot is capable to move or displace over a surface without falling and dodging the elements in the environment, like obstacles, people or both [3]. For this, two main features are necessary: a mechanical structure that allows the robot to move over almost any surface, and a

suitable sensor implementation to detect and avoid specific obstacles. For the first mentioned feature there are many developments of mobile robots with wheels, legs or both to have a suitable displacement over different kind of surfaces. Recently researches on mobile robots indicate that Hexapod Walking Robots (HWR) are being upgraded in their performance and motion capabilities by adding a wheel as end-effector (EE) to the extremity of each leg. These machines can move by using wheels, legs or both [4]. By combining both kinds of locomotion the robot is able to carry out a hybrid locomotion with complex paths and gaits to adapt to uneven surfaces or avoiding and overcoming different obstacles. Many advances have been developed in wheeled-legged robots, like the ATHLETE robot of the NASA, that have been designed to carry out extraterrestrial service tasks, such as, inspection and surveillance in Mars [5]. Another one is the shrimp robot, that has been developed at EPFL-Lausanne, and

✉ Daniele Cafolla, [contact@danielecafolla.eu](mailto:contact@danielecafolla.eu); [bioingegneria@neuromed.it](mailto:bioingegneria@neuromed.it); Giuseppe Carbone, [giuseppe.carbone@unical.it](mailto:giuseppe.carbone@unical.it) | <sup>1</sup>Instituto Politecnico Nacional, Querétaro, Mexico. <sup>2</sup>IRCCS Neuromed, Pozzilli, IS, Italy. <sup>3</sup>DIMEG, University of Calabria, Cosenza, Italy.



it can overcome vertical obstacles up to twice its wheel size and can even climb stairs [6]. There are other developments like the R3HC robot of the University of Huelva [7], or the ASTERISK of Osaka University [8]; that are robots for experimental research. There are also series of hybrid hexapod robots, like The Cassino Hexapod Series, that have been developed at the Laboratory of Robotics and Mechatronics (LARM) of the University of Cassino, to carry out several applications, including exploration of cultural heritage sites or performing helping tasks in hospitals. The Cassino Hexapod Robot III, the newest version of the Cassino Hexapod Robot series, is a six-wheeled-legged light-weight hybrid hexapod robot with a mecanum-wheel in each leg. This kind of wheels let it have an omni-directional displacement.

The hybrid configuration of Cassino Hexapod Robot III allows it to overcome little obstacles by using the legs, and to avoid bigger obstacles by using the mecanum-wheels. For the second mentioned feature for a suitable autonomy of a mobile service robot, there are many researches in the implementation of different strategies for obstacle recognition and avoidance by having a suitable sensor implementation of one, two or more different kind of sensors. In [9], it is reported Automated Area Surveillance Robot (AASR), a service robot with a 60fps camera, IR beamers and ultrasound sensors for human detection during a surveillance operation. Such robot is mainly designed for military operations and inspection tasks of facilities in companies. In [10], it is reported an autonomous neuronal controller for autonomous robots, where a behavior initiator to handle sensor activities for a high level of interaction and information exchange with humans is proposed. Such behavior initiator is basically a module of embedded sensors. Most of the sensors implemented in a robot for service operations are cameras and ultrasound sensors, this, to increase their motion autonomy and object recognition. For example, in [11], an algorithm for face recognition

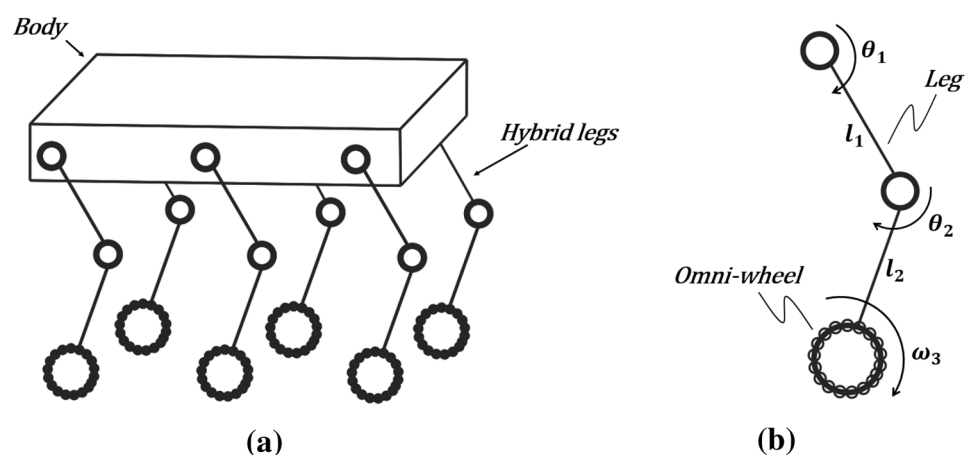
using sparse interest points in smart surveillance robots is proposed. The aim of this paper is to present the experimental validation of a proposed obstacle avoidance strategy, with Cassino Hexapod III, for different service operations, such as, surveillance and inspection, help or guidance inside a hospital. It is discussed the implementation of a RP-LIDAR sensor for obstacle recognition, as well as the feasibility and effectiveness of the proposed strategy.

## 2 Cassino Hexapod III: features and characteristics

Cassino Hexapod III is the latest version of the Cassino Hexapod Series, a family of wheeled-legged hexapod robots that haven been designed and built at LARM laboratory in Cassino since 2000. The main feature of this family of robots is low-cost and user-friendliness as based on a combinations of legs and wheels aimed to the inspection and operation at non-accessible sites, such as Montecassino Abbey, as well as surveillance, helping or guidance tasks in hospitals, such as IRCCS NEUROMED. Cassino Hexapod III is a wheeled-legged hexapod robot, Fig. 1a, with an omni-wheel in each leg as EE, Fig. 1b. Such omni-wheel is a mecanum wheel, which means their rollers are attached to the wheel circumference with an axis of rotation of  $45^\circ$  to the plane of the wheel [12], Fig. 2. This robot has a light-weight 3D printed body, on which six hybrid legs are attached to its chest. Its body can fit into a box of  $375 \times 230 \times 200$  mm, that allows to have two frontal legs, two lateral legs (one on each side), and two rear legs; all of them in frontal orientation, Fig. 3a.

Each hybrid leg consists in three servomotors, two of them ( $180^\circ$  servomotor) to actuate the pure motion of the leg, and the third one (continuous rotation servomotor), to actuate the motion of an omni-wheel, Fig. 3b. This

**Fig. 1** Wheeled-legged hexapod robots: **a** a general scheme [3], **b** a hybrid leg with an omni-wheel [3]



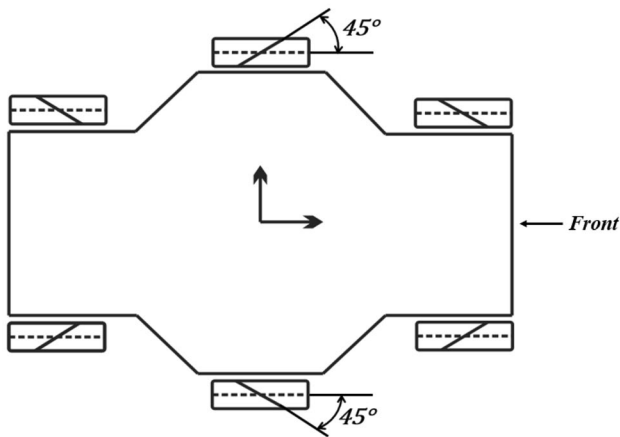


Fig. 2 Orientation of the omni-wheels in Cassino Hexapod III [3]

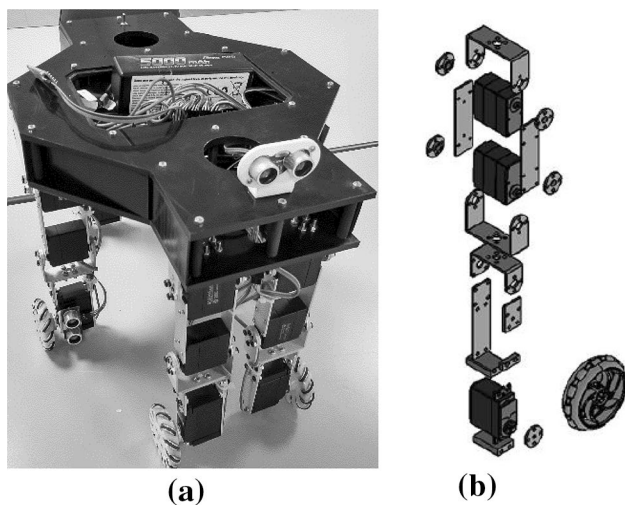


Fig. 3 Cassino Hexapod III: **a** photograph of the robot; **b** one hybrid leg [15]

kind of legs allows to carry out displacements along any direction over flat surfaces. The implementation of omni-wheels instead of common wheels in the hybrid legs is to easily avoid large obstacles by just rolling to any place along a straight line, or to overcome small obstacles by carrying out complex motion with the combination of the motion of legs and wheels using the kinematic and strategy described in [13]. The control hardware of Cassino Hexapod III is fully onboard. It consists in an Arduino MEGA as the servo-controller, a servo-shield to connect the eighteen servomotors, and a Li-Po battery (Full Power 4S) with a regulator to decrease the voltage to 5 V [14], Fig. 4.

One of the main features of Cassino Hexapod III is its capability to move or displace over different kind of surfaces, such as, flat surfaces and rough ones. This feature

allows it to carry out different service tasks where is necessary to move faster with wheeled locomotion over a flat surface; or to move slower, but with greater security [16]. Furthermore, with legged locomotion, it can face rough terrains, or to avoid and overcome obstacles by rising one or more legs during a wheeled displacement. This feature of the robot is well presented in [14, 17], where the feasibility of a wheeled, legged, and wheeled-legged locomotion is discussed. Since the robot has mecanum wheels, it is also able to carry out complex displacements, where the robot can follow a circular gait without changing its local  $x$  or  $y$  local axis. Two new sensors have been embedded in the prototype to improve the orientation control and the obstacle and people avoidance strategies. For the former strategy an IMU sensor has been embedded in the platform as a feedback of its angular displacement; it has a MPU6050 device combined with a 3-axis gyroscope and a 3-axis accelerometer on the same silicon together with an onboard Digital Motion Processor (DMP) capable of processing complex 9-axis Motion Fusion algorithms [2]. Furthermore, it is very small size of  $22 \times 17 \times 15$  mm and low weight of 6 g, making it perfect for a portable device [18]. For precision tracking of both fast and slow motions, the parts feature a user-programmable gyro full-scale range of up to  $\pm 2000^\circ/\text{s}$  (dps) and a user-programmable accelerometer full-scale range up to  $\pm 16$  g. For the latter mentioned strategy a LIDAR sensor has been chosen for Bi-dimensional  $360^\circ$  real-time with its weight of 170 g and its low power-consumption of 2.5 W. The Bi-dimensional real-time mapping is based on laser triangulation ranging principle and uses high-speed vision acquisition and processing hardware. The system measures distance data in more than 8000 times per second [19]. These new characteristics improve the already validated performance of Cassino III Hexapod with its linear velocity while rolling of 14.16 cm/s, and while walking of 2.22 (cm/s); its average angular displacement over  $z$  axis of  $1.18^\circ$  and its energy autonomy of 3.5 h.

### 3 Obstacle avoidance strategy

The obstacle avoidance strategy is designed for service operations of surveillance, hosting or guidance inside hospitals. In this case, it is specially designed for the mentioned tasks inside IRCCS NEUROMED hospital in Pozzilli, Italy. The main idea is to detect if any patient is having a trouble or if there is happening something wrong in a specific area of the hospital, to guide the patient from a location to another, or simply carry needed object from a site to another. The layout of the obstacle avoidance strategy is presented in Fig. 5. In this strategy, the robot is moving forward, and when it recognize a person or any

**Fig. 4** Cassino Hexapod III schematic diagram of the hardware control

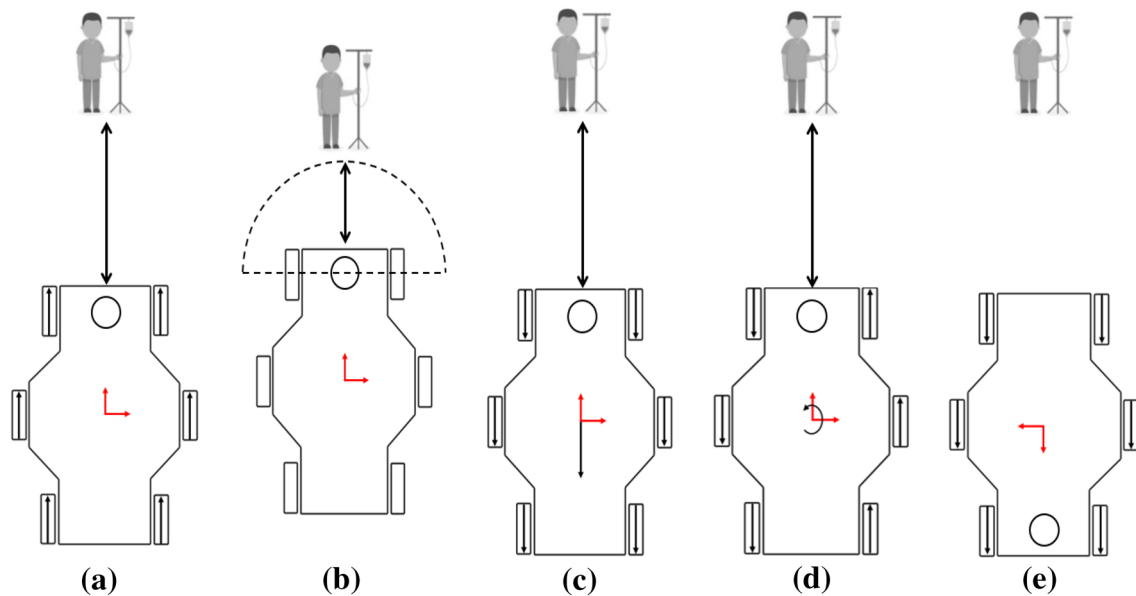
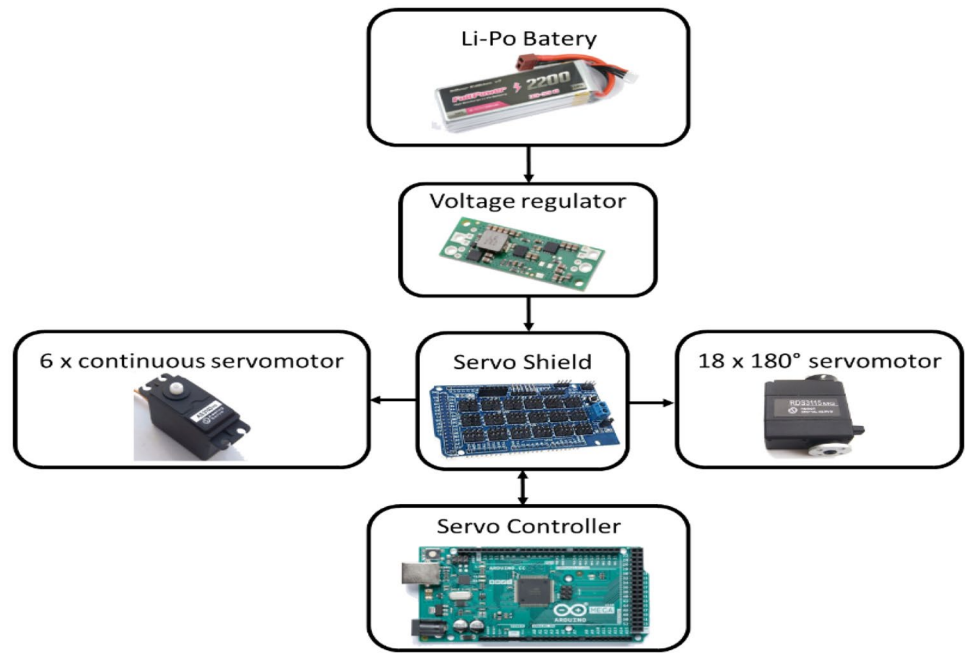


**Fig. 5** Layout of the proposed obstacle avoidance strategy

other obstacle it stops for few seconds to validate that the obstacle continues there; then the robot turns 180° to its back and continue moving forward, avoiding an obstacle in front of it.

### 3.1 Sensors implementation

The sensors implementation is performed for two main cases: the first, the use of an ultrasonic sensor, and the

second, a RP LIDAR. Both sensors are able to sense the distance between an object in front of them by using a specific operation principle and technology. In the first case, the ultrasonic sensor measures the distance by calculating the time between a high-frequency sound signal sent by the transmitter and its reception at the receiver, after it is reflected by an object. In the second case, the RP LIDAR measures the distance and the polar position of an object by emitting a modulated infrared

laser signal, when this signal is reflected by an object, a vision acquisition system sample the returning signal and it is processed to obtain the distance and angle values between the object and the RP LIDAR. By implementing both sensors for a simulated service operation, their performance and results can be compared.

### 3.1.1 Ultrasonic sensor

The ultrasonic sensor implementation is carried out with a different obstacle avoidance strategy from the proposed one, since this sensor only can measure the distance between an object and the robot, but not the quantity of objects and their size. For this case, it is proposed the operation strategy of Fig. 6a), where the robot is rolling forward, and it stops when an object is sensed in 150 mm or less, then, the obstacle avoidance strategy starts. The obstacle avoidance strategy, Fig. 6b), starts with an omnidirectional displacement of the robot, until its Center of Mass (CoM) displaces 90°, then the robot stops and starts to turn 90° counter-clockwise over its own axis, and it finishes the avoidance strategy by stopping. After the obstacle avoidance strategy finishes, the robot continues rolling forward and sensing for a new obstacle. Ultrasonic sensor is mounted in the front of the robot, see Fig. 7. The connection schematic diagram of the sensor is presented in Fig. 8. An Arduino Nano is used as data acquisition interface for ultrasonic sensor. The acquired data is sent to the servo controller of Cassino Hexapod III to carry out the obstacle avoidance strategy; it is also sent to a PC via Bluetooth, with a HC-05, to save the real-time data of the sensor for further post-processing.

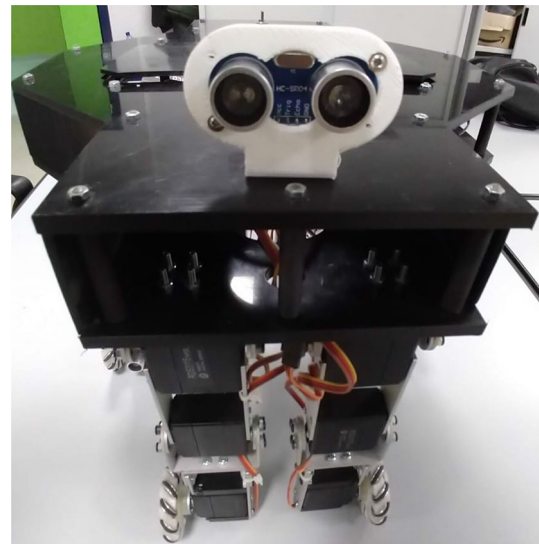
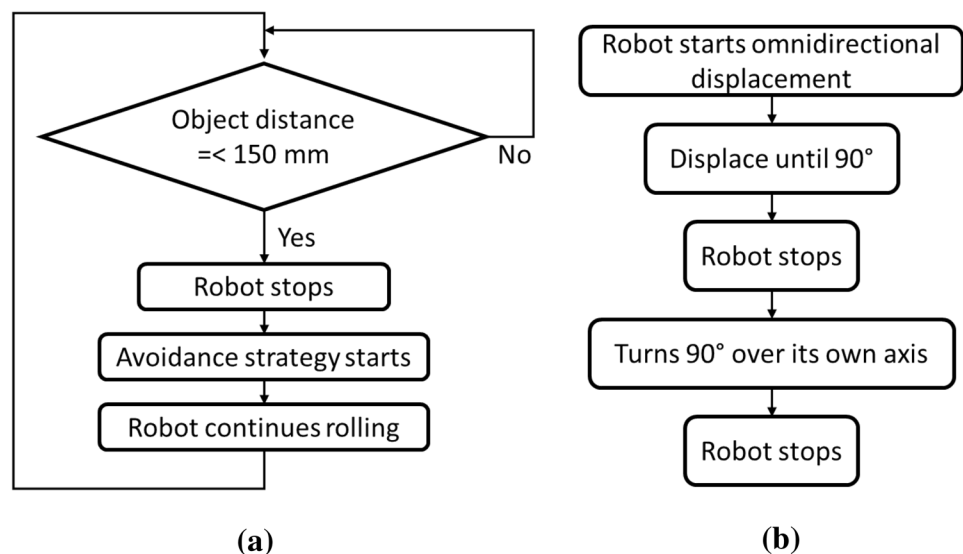


Fig. 7 Ultrasonic sensor mounted on Cassino Hexapod III

### 3.1.2 RP LIDAR sensor

The RP LIDAR sensor implementation is carried out to test the proposed obstacle avoidance strategy to dodge people and objects during a service operation, like surveillance, in IRCCS NEUROMED hospital in Pozzilli. The sensor is mounted over the frontal part of Cassino Hexapod III, Fig. 9, so that the sensor can detect any object in front of the robot. The sensor data acquisition system is fully onboard with the control system of the robot, and it consist of an Arduino MEGA as DAQ. The connection schematic diagram for RP LIDAR and its DAQ system is presented in Fig. 10, where it can be appreciated that the sample data of the sensor is sent to the servo controller of the robot

Fig. 6 Obstacle avoidance strategy for using an ultrasonic sensor: **a** operation strategy, **b** avoidance strategy



**Fig. 8** Connection schematic diagram for the ultrasonic sensor

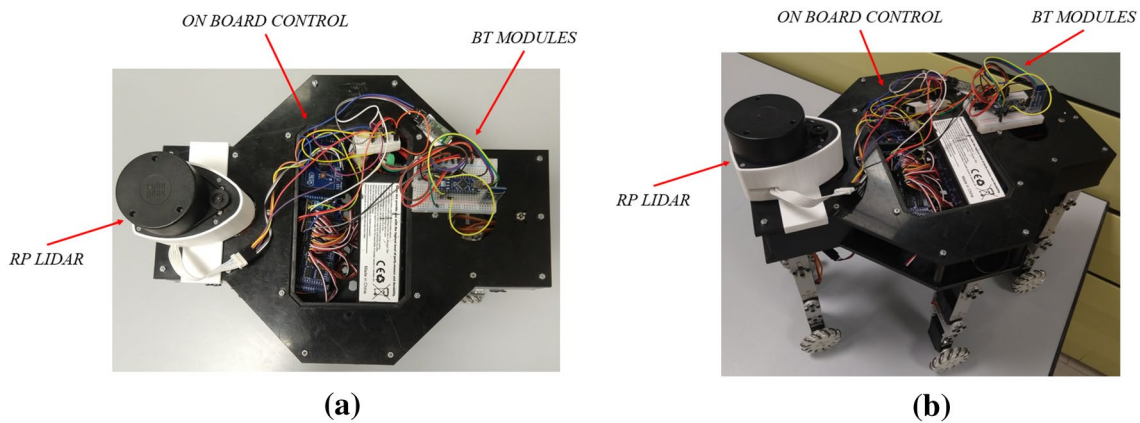
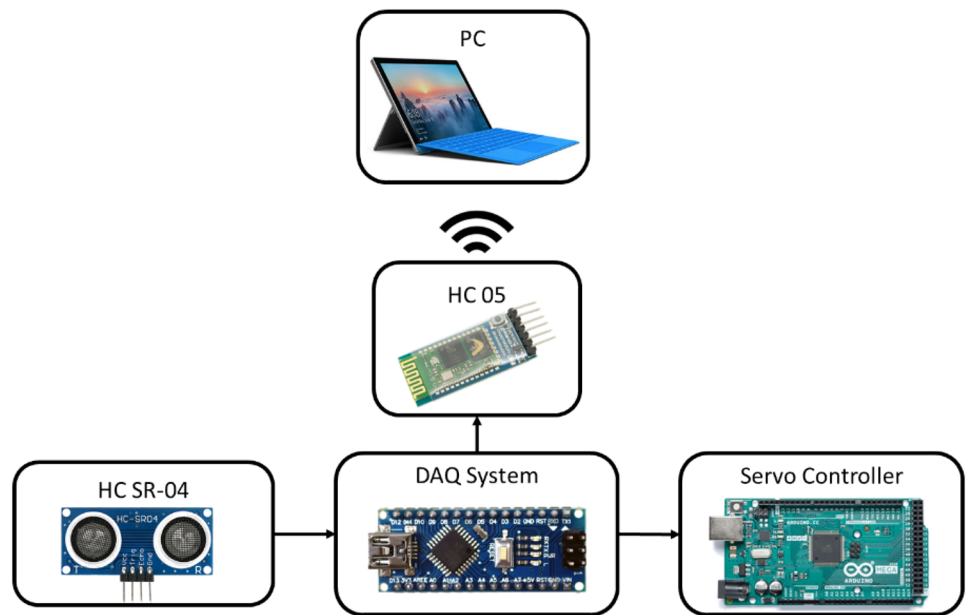


**Fig. 9** RP LIDAR mounted over Cassio Hexapod III: **a** top view, **b** isometric view

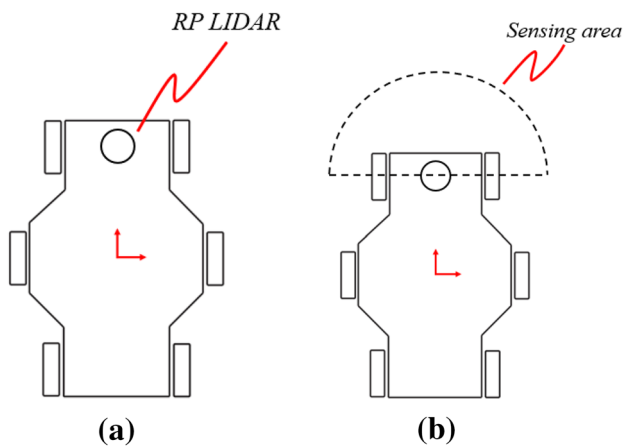
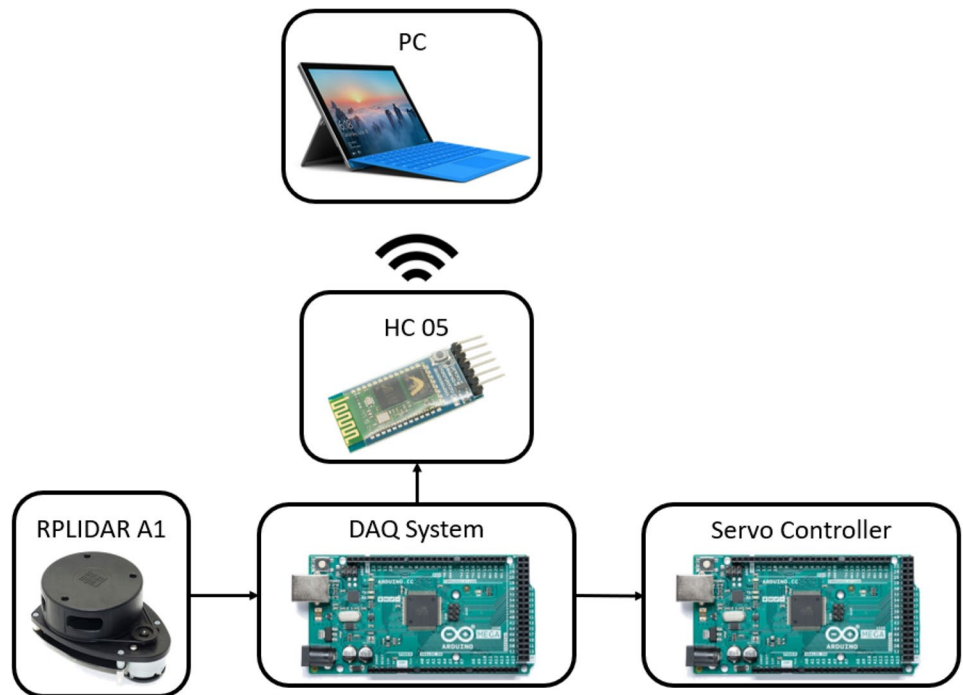
and to a PC via Bluetooth. On one hand, the data is sent to the servo controller, where the obstacle avoidance strategy is embedded, so the robot can take a decision about its locomotion; on the other hand, the data is sent to a PC for a visual representation of the acquired sample data. In Fig. 11, the mounting position of the RP LIDAR over Cassio Hexapod III, and its sensing area is presented. Since the RP LIDAR is in a continuous rotation and it can sense objects around 360°, the sensing area is delimited to only a part of the whole sensing range, Fig. 11b). Thus, the sensing area is delimited to a range of 270°–90° (total of 180°) with a radius of 800 mm, by this way the sensor is able to detect objects only in the frontal part of the robot.

Before starting any service operation or experimental test for the obstacle avoidance strategy, the functionality

of RP LIDAR has been tested by carrying out an experimental test of mapping. Such test consists in mapping the area in front of the robot without considering any limitation in the sensing radius distance. Three different objects are positioned in front of the robot for mapping, from left to right: a carton box, a tool cart, and a wooden table, Fig. 12.

The results of the experimental test of mapping are presented in Fig. 13. It is possible to notice the location of the objects surrounding the robot, the groups of points represent the faces of the object. Comparing Figs. 12 and 13 it can be noticed that the sensing points represents the real configuration. Since the acquired sample data is obtained in polar coordinates, it is presented the overlay in polar coordinates of the mapping in Fig. 13a). In such overlay is appreciable that the three objects are inside of the proposed

**Fig. 10** Connection schematic diagram for the RP LIDAR sensor

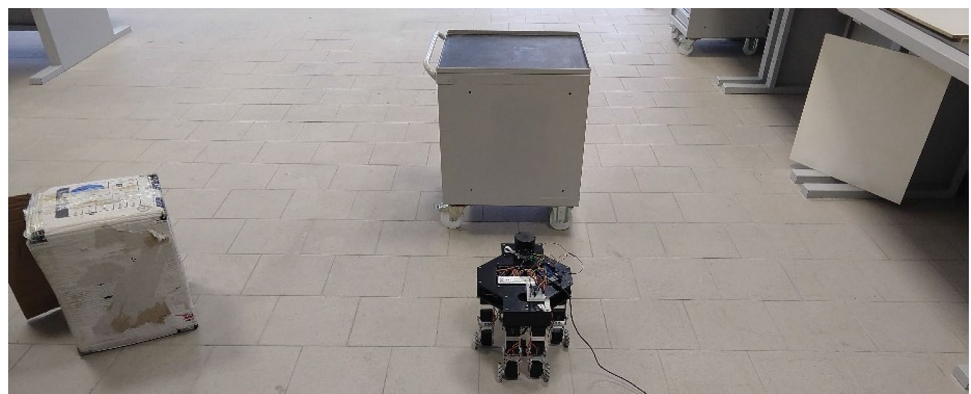


sensing range, from 270° to 90°, and that their positions at the graphic correspond to the real positions of the test. To have a better appreciation of this, the polar coordinates have been converted to cartesian coordinates. Also, it is necessary to apply the rotation matrix for y axis (1), since the acquired data is in mirror view due to the image acquisition of the RP LIDAR camera. The result of conversion is presented in Fig. 13b). In such figure, it is easy to appreciate in a cartesian space the position of the three different objects that are sited in front of the robot.

$$R_y(\theta) = \begin{bmatrix} \cos \theta & 0 & \sin \theta \\ 0 & 1 & 0 \\ -\sin \theta & 0 & \cos \theta \end{bmatrix} \tag{1}$$

**Fig. 11** RP LIDAR on Cassino Hexapod III: **a** sensor over hexapod robot, **b** sensing area of RP LIDAR

**Fig. 12** Experimental test for RP LIDAR for mapping the different objects in front of Cassino Hexapod III



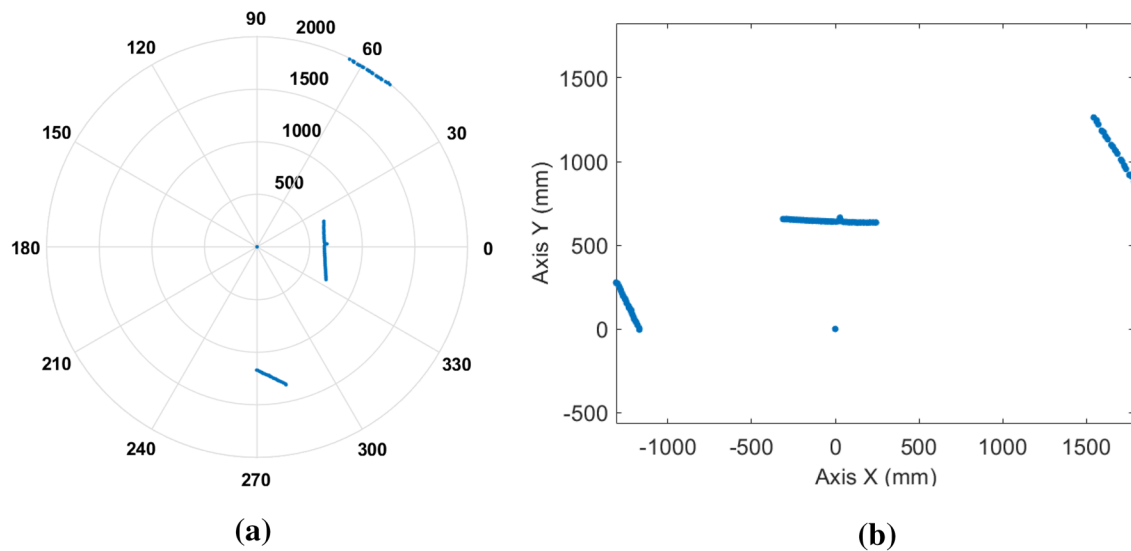
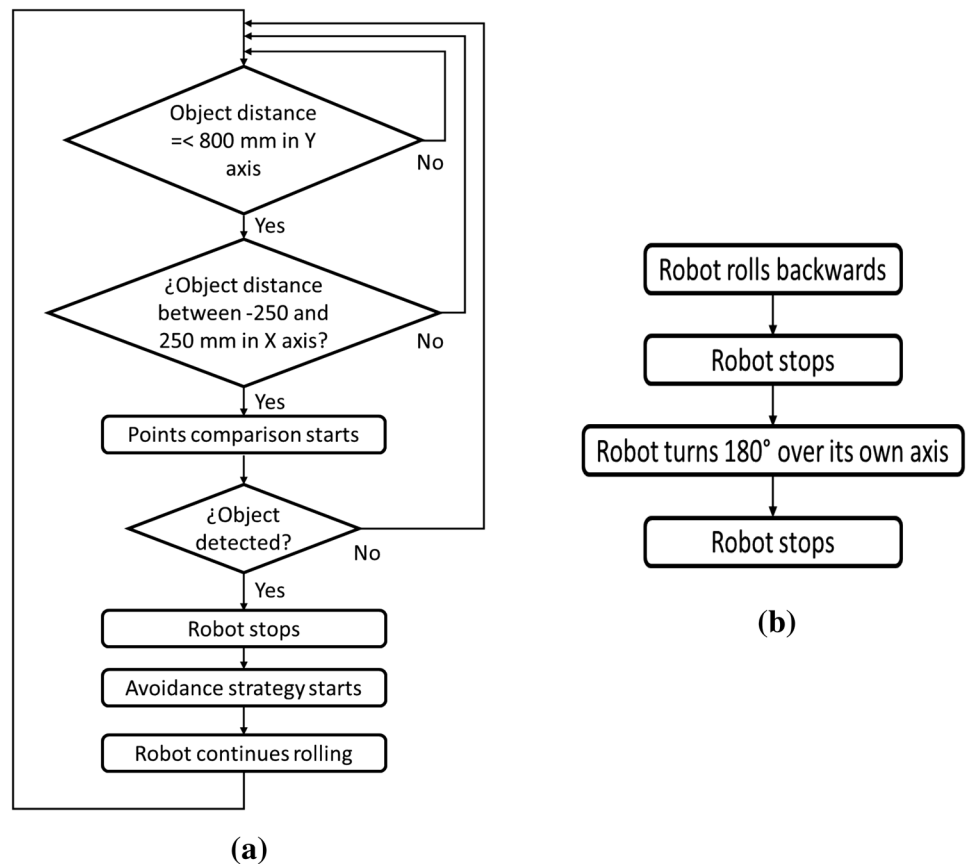


Fig. 13 Experimental results of the test for RP LIDAR, position of the mapped objects: **a** in polar coordinates, **b** in cartesian coordinates

To validate the obtained data from the RP LIDAR, the average dimension from the robot to the central object, the tool cart has been compared. The average obtained distance is 622 mm and the average measured distance is 626 mm.

The operation strategy for the proposed obstacle avoidance strategy is presented in Fig. 14. This operation strategy is embedded in the servo controller of Cassino Hexapod III. According with Fig. 14, if the RP LIDAR detects a point of an object in a distance less than 800 mm in the y

Fig. 14 Obstacle avoidance strategy for using RP LIDAR: **a** operation strategy, **b** avoidance strategy





axis, and, between  $-250$  and  $250$  mm in the  $x$  axis, taking in account that  $0$  mm of the  $x$  axis is in the center of the RP LIDAR, the points comparison starts. The points comparison allows to detect if the sensed points are part of a single object or, if they are part of different objects. Thus, the points comparison detects the continuity of the detected points by adding up the points detected in the same area. When the comparison determinates an object is in front of the robot, the robot stops, and the obstacle avoidance strategy starts. According to Fig. 14b), the obstacle avoidance strategy consists in rolling backward, for 3 s, and then stop, and turn  $180^\circ$  over the own axis of the robot, using

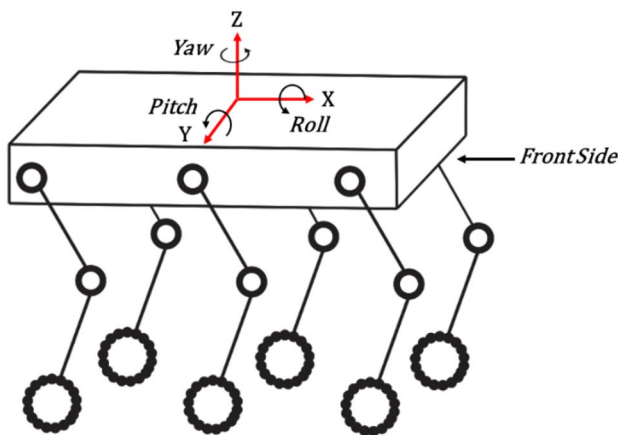
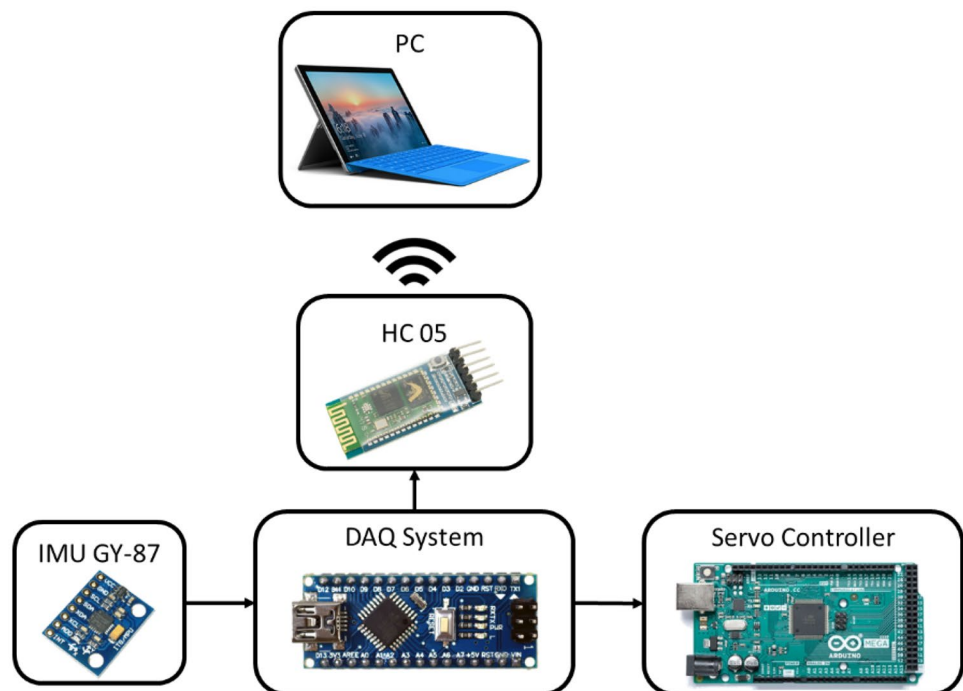


Fig. 15 IMU reference coordinate system on Casino Hexapod III

Fig. 16 Connection schematic diagram for the IMU sensor



differential traction, and finally stops again to continue the operation strategy.

### 3.1.3 IMU sensor

The IMU sensor implementation is performed to obtain the angular position of the robot in real-time. IMU sensor is mounted over the middle of the robot chest. The reference coordinate system of the IMU is presented in Fig. 15. In such figure, each axis and its corresponding angle of the reference coordinate system. For the obstacle avoidance strategy is important to measure the *Yaw* angular displacement, thus, the robot is able to stop in the correct angular position. To implement the IMU sensor, an Arduino Nano as DAQ system has been used. In such DAQ system, it is embedded an auto-calibration process for the IMU, so that it is ready to use every time the robot is started. A connection schematic diagram of the IMU is presented in Fig. 16. According with such figure, the DAQ system sends the sample data to the servo controller, and to a PC via Bluetooth. The signal is sent to the servo controller to control the behavior of the robot during the avoidance strategy; and to a PC for a further post-processing.

## 4 Experimental validation

To evaluate and experimentally validate the proposed operation strategies for obstacle avoiding, a simulated service task within a hospital facility is proposed. The chosen

simulated service task is to avoid people and/or objects without losing sight of them avoiding unwanted injuries. The robot maintains a distance within a security range, when the person or obstacle is avoided it turns around and distances itself from the warning area. The simulated service task is carried out at Biomechatronics Lab at the Technological Park of IRCCS NEUROMED in Pozzilli, Italy.

### 4.1 Ultrasonic sensor

In Fig. 17, the layout for the experimental validation of the proposed operation strategy with an ultrasonic sensor is presented. In such figure, it can be noticed that the robot moves forward in straight line and stop fifteen centimeters of a wall. After the robot senses the wall, it waits 2 s to stabilize its body, and then starts an omni-wheeled

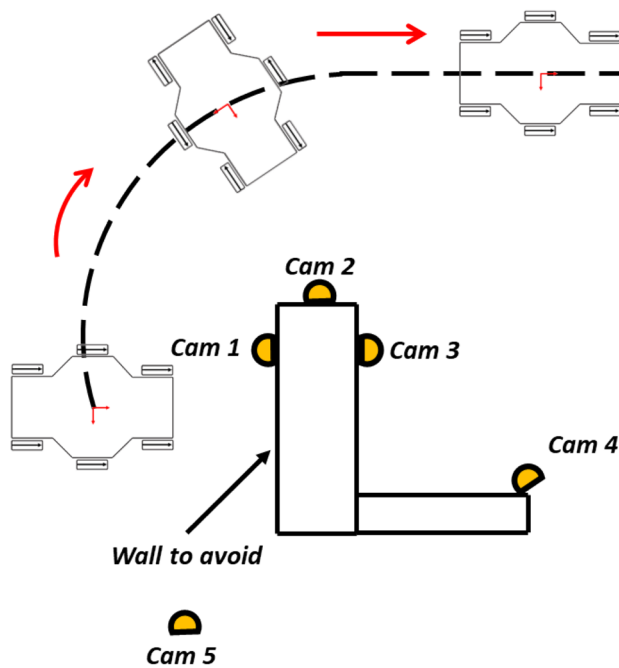


**Fig. 17** Layout of the experimental test to avoid a wall using an ultrasonic sensor

locomotion of one quarter of a circular trajectory. Thus, the robot will be on the side of the wall. After this, the robot will wait 2 s to stabilize the body and then turn 180° around its own axis and start again a forward straight displacement. Also, the cameras position to video record the experimental test is presented in Figs. 17 and 18 presents a photo sequence during the experimental test with Casino Hexapod III, where four cameras are used to capture different points of view. The test results are presented in Fig. It can be noticed, Fig a), that the robot stopped in the set condition, 148.7 mm, furthermore the displacement is linear until the robot sensed the wall. In Fig b) is presented the comparison between the target and the real avoidance gait, where is possible to appreciate the error between them. In this case, it is shown that the robot has a delay to start the avoidance gait, and that also the robot took more time to reach the first value of the target, with a minimal overshoot of 2.40°. Also, it is appreciated that both gaits finished almost at the same time, with a difference of 0.78 s, an overshoot of -0.33° and an average angular speed of 15.33°/s. The average measured values are presented in Table 1 and the test is shown in Fig. 19.

### 4.2 RP LIDAR sensor

For the experimental validation of the proposed operation strategy for obstacle avoiding using a RP LIDAR, the robot is leaved in the laboratory with two people walking around it, thus the robot must sense and recognize them, as well as the objects in its surround. Figure 20 presents moments where the robot has detected an obstacle in the security range, in this case the people, and it started the operation strategy. Figure 20a, b shows

**Table 1** Average measured values of the proposed simulated task for an obstacle avoidance strategy for service operations using an ultrasonic sensor

Trajectory final error in yaw	Stopped distance (mm)	Angular speed (°/s)	Linear speed (mm/s)
-0.33°	148.7	15.33	91.4

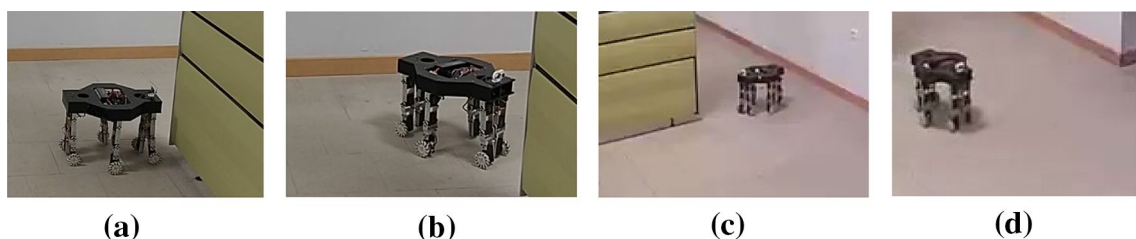


**Fig. 18** Photo sequence of the experimental test for obstacle avoidance using an ultrasonic sensor: **a** robot stops in front of the wall, **b** robot starts the avoidance gait, **c** the robot stops, **d** robot starts again straight forward displacement

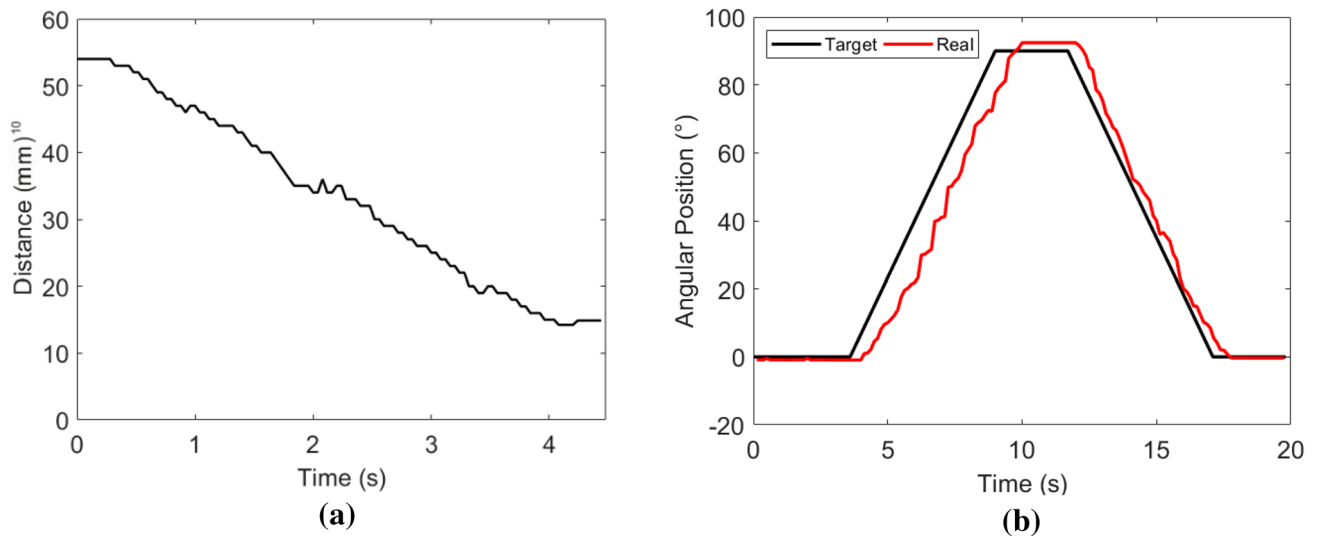


**Fig. 19** Test results: **a** linear displacement of the robot before it started the avoidance gait, **b** comparison between target and real angular displacements of CoM

the experimental environment with the robot and the people. Figure 20c, d presents the real-time acquired data with the RP LIDAR and a graphic interface developed with Processing software. In Fig. 20e, f the post-processed acquired data is presented. It is important to emphasize that in both moments the legs of the people were sensed and shown in the plot, and that sensed points are inside of the measure range. Furthermore, it can be seen that the graphics of the real-time acquired data and the post-processed data are almost equal. The test result is presented in Fig. 21; the figure presents the comparison between the target and the real avoidance gait, where it is possible to appreciate the error between them. In this case, it is shown that the robot has a delay to start the avoidance gait, and that also the robot took more time to reach the set value of the target, with a minimal overshoot of  $2.10^\circ$ . In addition, it can be noticed that both gaits finished almost at the same time, with a difference of 0.54 s and an average angular speed of  $40.73^\circ/\text{s}$ .

By comparing the test results by both sensors, it can be appreciated, since the RP LIDAR can give a higher precision to detect the obstacle and its size, that the implementation of the operation strategy, as well as the performance of the RP LIDAR sensor, is superior to the ultrasonic sensor for an obstacle avoidance for a service operation with human interaction.

Finally, Table 2 Resumes the performances of the prototype during the experimental campaign. These

characteristics show a very high autonomy and satisfactory results required for the desired task.

## 5 Conclusions

This paper reports a successful experimental validation of an obstacles avoidance strategy that has been specifically developed for a complex human-shared environment. The proposed strategy refers to a hardware composed of a hybrid legged-wheeled hexapod robot with sonar, IMU and RP Lidar sensor feedback. A wireless acquisition system has been successfully developed to detect the objects in front of the robot, and to measure their distance and orientation from the robot. The main merit of the proposed strategy is the versatility to cope with several obstacles as well as the increased autonomy in unpredictable environments as also demonstrated by preliminary tests in a hospital environment. The presented strategy is sensor-based strategy using pre-established trajectories while maintaining safety distances with pre-set safety parameters. Operation strategies and paths, which can benefit from omni-wheels in complex human-shared environment proved their effectiveness avoiding obstacle and always maintaining the pre-set safety distance. Furthermore, the prototype has proved is high grade of portability due to its very light weight and optimal autonomy.

Future work will systematically test the proposed method in clinical environment implementing the

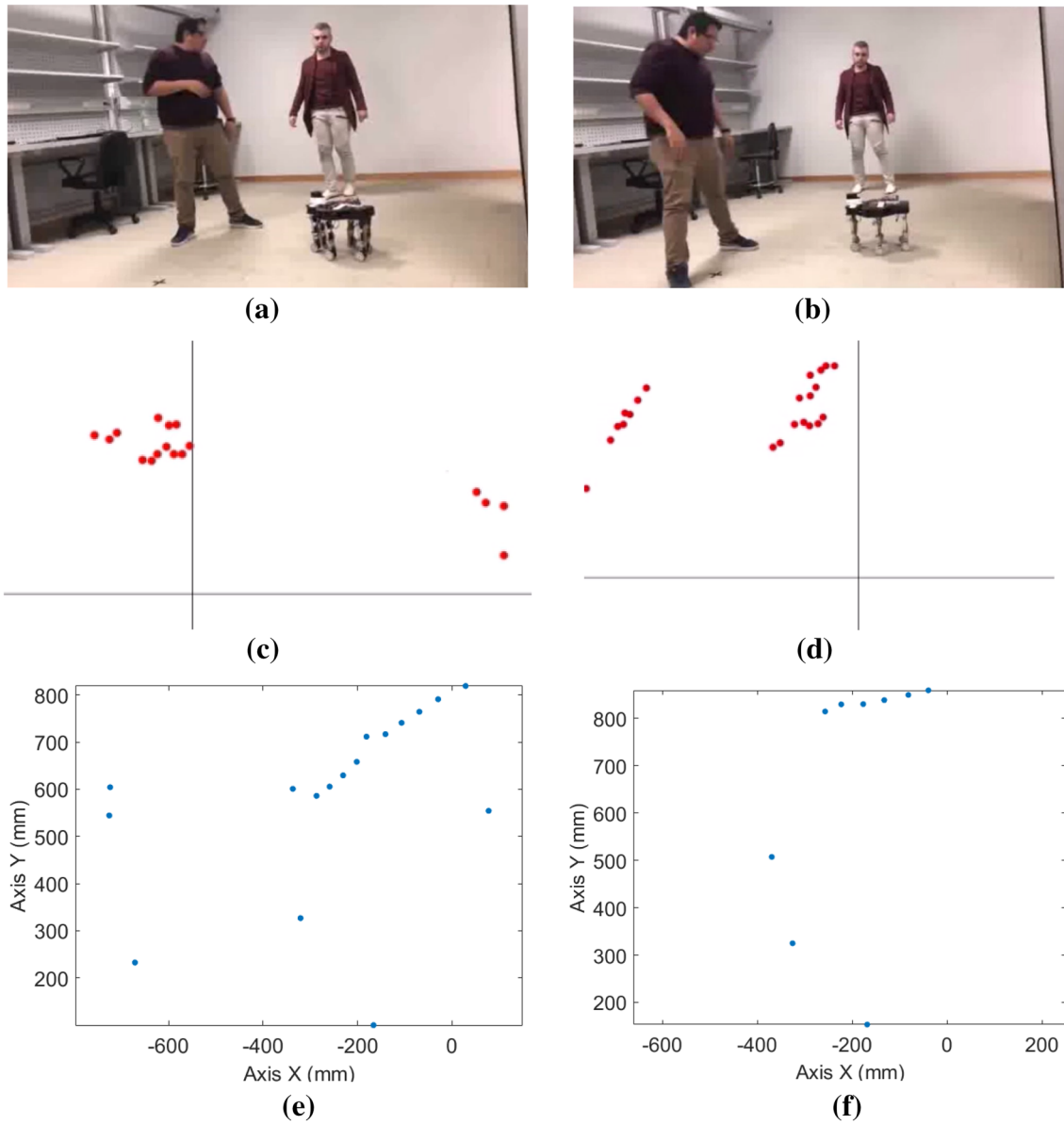


**Fig. 20** Acquired data of two moments during the experimental test for obstacle avoiding strategy by using a RP LIDAR: **a** photo of the first moment; **b** photo of the second moment; **c** plot of the real-time acquired data during the first moment, **d** plot of the real-

time acquired data during the second moment, **e** plot of the post-processed acquired data of the first moment, **f** plot of the post-processed acquired data of the second moment

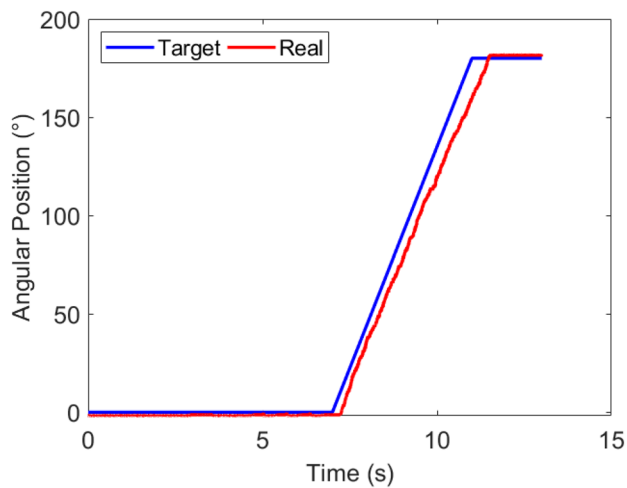


**Fig. 21** Comparison between target and real angular displacements of CoM during the experimental test

**Table 2** Average measured values of Cassino Hexapod III performances

Steering radius (mm)	Angular speed (°/s)	Linear speed (mm/s)	Maximum step high (mm)	Autonomy (h)	Weight (kg)
800	40.73	91.4	60	>2.25	≈ 3

proposed operation strategy for several tasks such as surveillance patrolling and/or patient guidance.

**Acknowledgements** The first author wishes to thank ACRI association for grants which supported him for period of study at LARM in Cassino within 2018 under the supervision of Prof. Giuseppe Carbone.

### Compliance with ethical standards

**Conflict of interest** The authors declare that they have no conflict of interest.

### References

1. Franco T, Carbone G (2016) A legged robotic system for remote monitoring. In: *New trends in medical and service robots*, pp 221–231
2. M. Ceccarelli, D. Cafolla, M. Russo and G. Carbone (2018) HeritageBot platform for service in cultural heritage frames. *Int J Adv Robot Syst* 1–13

3. Orozco-Magdaleno EC, Cafolla D, Castillo-Castañeda E, Carbone G (2019) Experimental validation of a gait planning for obstacle avoidance using mecatronic wheels. In: *Proceedings of the 15th IFTOMM world congress*
4. Bares J, Hebert M, Kanade T, Krotkov E, Mitchell T, Simmons R, Whittaker W (1989) Ambler: an autonomous rover for planetary exploration. *IEEE Comput* 6–18
5. Tedeschi F, Carbone G (2015) Design of hexapod walking robots: background and challenges. In: *Handbook of research on advancements in robotics and mechatronics*, pp 527–566
6. Estier T, Piguet R, Eichhorn R, Siegwart R (2000) Shrimp: a rover architecture for long range martian mission. In: *Proceedings of the sixth ESA workshop on advanced space technologies for robotics and automation (ASTRA)*
7. Gomez-Bravo F, Villadoniga P, Carbone G (2018) Design and operation of a novel hexapod robot for surveillance tasks. In: *Design and operation of a novel hexapod robot for surveillance tasks*, pp 707–715
8. Ysushi M, Yuuya T, Tatsuo A, Kenji I, Norihiro K (2004) Omni-directional locomotion of robots with limb mechanism. *J Robot Soc Jpn*, 329–335
9. Ganeshanand B, Soorya S, Hari-Krishna-Menon S (2015) Automated area surveillance robot (AASR). *Int J Sci Eng Res (IJSER)*, 431–434
10. Chang O (2018) Autonomous robots and behavior initiators. In: *Human-robot interaction—theory and application*, pp 125–141
11. Vinay A, Sai-Krishna BV, Manoj PN, Nishanth AR, Balasubramanya KN, Nataranja S (2018) Person identification in smart surveillance robots using sparse interest points. In: *Procedia computer science* 133 ROSMA, pp 812–822
12. Taheri H, Qiao B, Ghaeminezhad N (2015) Kinematic model of a four mecanum wheeled mobile robot. *Int J Comput Appl* 113(3):6–9
13. Tedeschi F, Carbone G (2017) Design of a novel leg-wheel hexapod walking robot. *Robotics* 6(4):40
14. Orozco-Magdaleno EC, Cafolla D, Ceccarelli M, Castillo-Castañeda E, Carbone G (2018) Experiences for a user-friendly operation of Cassino Hexapod III. In: *Proceedings of 27 RAAD conference*, pp 205–213
15. Tedeschi F, Cafolla D, Carbone G (2014) Design and operation of Cassino Hexapod II. *Int J Mech Control* 15:19–25
16. Carbone G, Tedeschi F, Gallozi A, Cigola M (2015) A robotic mobile platform for service tasks in cultural heritage. *Int J Adv Robot Syst* 1–10
17. Orozco-Magdaleno EC, Carbone G, Castillo-Castañeda E (2018) Experiences on a hybrid locomotion approach to overcome obstacles with Cassino Hexapod III. In: *de Proceedings of 2nd IFTOMM Italy conference*, pp 1–8
18. Invensense (2013) “MPU 6000”. <https://www.invensense.com/wp-content/uploads/2015/02/MPU-6000-Register-Map1.pdf>. Accessed 2018
19. RoboPeak Team (2014) “Robotshop”. <https://www.robotshop.com/media/files/pdf/user-manual-rplidar.pdf>. Accessed 2018

**Publisher’s Note** Springer Nature remains neutral with regard to jurisdictional claims in published maps and institutional affiliations.